Advantage of suppressed non-Langevin recombination in low mobility organic solar cells

Martin Stolterfoht, Bronson Philippa, Ardalan Armin, Ajay K. Pandey, Ronald D. White, Paul L. Burn, Paul Meredith, and Almantas Pivrikas

Citation: Applied Physics Letters **105**, 013302 (2014); doi: 10.1063/1.4887316
View online: http://dx.doi.org/10.1063/1.4887316
View Table of Contents: http://scitation.aip.org/content/aip/journal/apl/105/1?ver=pdfcov
Published by the AIP Publishing

Advantage of suppressed non-Langevin recombination in low mobility organic solar cells

Martin Stolterfoht,[1] Bronson Philippa,[2] Ardalan Armin,[1] Ajay K. Pandey,[1] Ronald D. White,[2] Paul L. Burn,[1] Paul Meredith,[1] and Almantas Pivrikas[1,a)]
[1]*Centre for Organic Photonics & Electronics (COPE), School of Chemistry and Molecular Biosciences and School of Mathematics and Physics, The University of Queensland, Brisbane 4072, Australia*
[2]*School of Engineering and Physical Sciences, James Cook University, Townsville 4811, Australia*

(Received 12 December 2013; accepted 24 June 2014; published online 8 July 2014)

Photovoltaic performance in relation to charge transport is studied in efficient (7.6%) organic solar cells (PTB7:$PC_{71}BM$). Both electron and hole mobilities are experimentally measured in efficient solar cells using the resistance dependent photovoltage technique, while the inapplicability of classical techniques, such as space charge limited current and photogenerated charge extraction by linearly increasing voltage is discussed. Limits in the short-circuit current originate from optical losses, while charge transport is shown not to be a limiting process. Efficient charge extraction without recombination can be achieved with a mobility of charge carriers much lower than previously expected. The presence of dispersive transport with strongly distributed mobilities in high efficiency solar cells is demonstrated. Reduced non-Langevin recombination is shown to be beneficial for solar cells with imbalanced, low, and dispersive electron and hole mobilities. © *2014 AIP Publishing LLC*. [http://dx.doi.org/10.1063/1.4887316]

Recently, the power conversion efficiencies (PCEs) of prototypical bulk heterojunction (BHJ) organic solar cells (OSCs) have exceeded 10%, with these performance improvements delivered primarily through the development of new materials and improved device architectures. In order to make further progress, it is imperative to clarify the critical processes that limit the PCE. While efforts are continuing to improve light harvesting and charge generation efficiencies, it is also vitally important to ensure the efficient transport of all the photogenerated mobile charges to the respective electrodes with minimal recombination losses.[1] Both charge carrier mobility and recombination strongly depend on the material properties and the film nano- and microstructure.[2] Therefore, when aiming to clarify the charge collection efficiency in OSCs, it is essential to accurately measure the electron and hole mobilities simultaneously with the bimolecular recombination coefficient in operational solar cells.

In this Letter, the charge carrier mobility and recombination are directly measured in efficient polymer-based solar cells by employing the Resistance dependent PhotoVoltage technique. The impact of significantly suppressed bimolecular recombination is studied with respect to the photo carrier mobility and charge extraction. The measured mobilities of both electrons and holes are compared to the values typically reported in the literature and correlated to the efficiency of the solar cells. Efficient charge extraction is demonstrated despite carrier mobilities that are much lower than is commonly thought to be necessary, because of the suppressed bimolecular recombination in the studied devices. Furthermore, we demonstrate the dispersion of the charge transport in operational solar cells.

The most popular techniques to measure charge transport in organic semiconductors are: Organic Field Effect Transistors (OFET);[3] Current-Voltage analysis using space charge limited current (SCLC) models;[4] Time-of-Flight (TOF);[5] and Charge Extraction by Linearly Increasing Voltage (CELIV).[6–8] Unfortunately, none of these techniques are generally applicable to operational OSC devices due to various experimental or device structure related restrictions.[1] For instance, charge carrier mobilities measured using OFETs often differ by orders of magnitude compared to the values measured in diodes.[9,10] This mismatch is attributed to the specifics of trap states of the semiconductor/insulator interface of the OFET channel as well as to the large difference in the carrier concentrations between the different device geometries.[9] Current-Voltage characteristics are typically applied to non-operational unipolar devices, while charge trapping, a signature of disordered transport, often hinders the interpretation.[11] Classical TOF mainly uses "thick" (several μm) organic semiconductor films while OSC junctions are typically in the hundreds of nanometers range. Strongly dispersive transport in disordered organic semiconductors smears out the time-of-flight transient and further limits the applicability of this technique.[5] Recently, we developed the Resistance dependent PhotoVoltage (RPV) technique,[12] which allows the electron and hole mobilities to be measured simultaneously in operational OSCs, directly from the transient signals without the need for fitting procedures. Moreover, numerous advantages of RPV have been demonstrated, such as robustness against: (a) interference governed light absorption profile; (b) bimolecular recombination; (c) circuit resistance; and (d) amount of trapped charge carriers.

The substrates (PEDOT:PSS/ITO/glass) were prepared as previously described in Ref. 13 and the active layer of PTB7 (1-material, $\bar{M}_w = 97.5$ kDa, PDI = 2.1) and $PC_{71}BM$ (ADS) as described in Ref. 14 using a total concentration of 31 mg/cm^3. This resulted in a film ~125 nm thick (measured using a DekTek profilemeter). Finally, 1.2 nm of samarium and 75 nm of aluminium were deposited under a 10^{-6} mbar

a)Author to whom correspondence should be addressed. Electronic mail: almantas.pivrikas@uq.edu.au

vacuum by thermal evaporation. The device area was 0.2 cm^2 for current density vs. voltage (*J-V*) and external/internal quantum efficiency (EQE/IQE) measurements, whereas a device area of 1 mm^2 was used for the RPV and photo-CELIV measurements.

J-V characteristics were obtained in a 4-wire source sense configuration and were nearly identical in a set of 8 devices (PCE ± 0.1%). An Abet Class AAA solar simulator was used as the illumination source providing ~100 mW/cm^2 of AM 1.5G light. The EQE spectrum was measured using a calibrated PV Measurements Inc. EQE QEX7 system. The IQE spectrum was obtained following a reported method[15] (see supplementary material[16]). RPV and photo-CELIV transients were recorded using our standard transient photoconductivity measurement setup.[12,17] An excitation wavelength of 532 nm was used to generate the charge carriers, while neutral optical density (OD) filters were used to attenuate the ~50 mJ energy output. In the case of photo-CELIV, the transients were obtained by using a triangular pulse length of 1 μs with a maximum applied voltage of 1 V and a load resistance (R_{load}) of 7.5 Ω. The RPV transients were measured without external voltage applied, and low laser pulse intensities (OD 7) were used for the mobility measurements to avoid space charge effects[12] (see supplementary material[16] for more details). In contrast, a high laser intensity (OD 3.5) was used to measure the bimolecular recombination coefficient on the same devices (see supplementary material[16] for more details).

Fig. 1(a) shows the white light AM 1.5 G *J-V* characteristics for typical PTB7:$PC_{71}BM$ devices. The high PCEs of

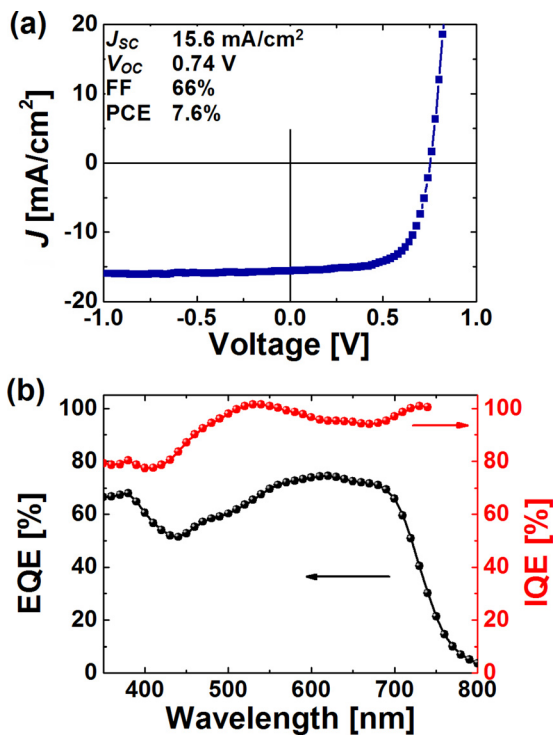

FIG. 1. (a) Current density versus voltage (*J-V*) characteristics of PTB7:$PC_{71}BM$ solar cells under AM 1.5 G illumination demonstrating high photovoltaic performance in a conventional device structure. (b) Typical EQE and IQE spectra. The difference arises from the light absorption losses within the device. The high IQE values across a broad wavelength range are observed as a result of efficient photocarrier generation and extraction – two essential processes for producing a large short-circuit current.

7.6% are comparable to previous reports of 7.4%[18] in a conventional device structure. In summary, average performance parameters were: open-circuit voltage (V_{OC}) = 0.74 V, fill factor (*FF*) = 66%, and short-circuit current density (J_{SC}) = 15.6 mA/cm^2.

The first step in elucidating the excellent performance of the devices and in particular the high J_{SC} was to measure the EQE and IQE spectra. As can be seen in Fig. 1(b), the IQE is almost 100% across the full wavelength range, indicating that both photogeneration and charge extraction are very efficient in this system. The fact that the EQE (~70%) is lower than the IQE originates from optical losses within the device[15] (see supplementary material[16]). Integration of the product of the EQE and the AM 1.5 G solar spectrum yields a calculated short-circuit current of 15.5 mA/cm^2, which matches with the J_{SC}, indicating negligible bimolecular recombination losses at 1 sun illumination.

In order to determine the charge transport parameters that are required to reach the observed high IQE values, we first tried to measure the carrier mobilities using the dark *J-V* characteristics by employing the SCLC model. According to the Mott-Gurney law, the SCLC is proportional to the square of the voltage.[19] However, this dependence was not observed in our measurements (see supplementary material[16]). Instead, the injection current appears to follow a linear dependence, which is governed by the series resistance of indium tin oxide (ITO).[20] This also demonstrates the general problem of the SCLC technique, namely, its inapplicability when: (a) the injection is limited by the series or contact resistance; or (b) charge transport is trap-limited. Even if the squared voltage dependence of the injection current is observed, there are multiple physical processes that can produce this functional dependence.[13,19] Furthermore, when the injection of one carrier type is blocked as proposed in Ref. 21 to measure the electron and hole mobilities separately, typically the injection of the other carrier type cannot be eliminated, especially at high applied electric fields. This issue becomes particularly important when measuring the slower carrier mobility in the case of strongly imbalanced transport.

In the past, photo-CELIV was applied to determine relatively low mobilities in organic photovoltaic systems with Langevin recombination.[22,23] The photo-current transients measured in the studied operational devices are shown in Fig. 2. Due to the short time scale of faster carrier extraction (~100 ns, visible in the RPV results presented later), the photo-response resembles an R_tC capacitive discharge (where R_t is the total circuit resistance and *C* is the device capacitance), which completely obscures the extraction maximum in the transient response of the photo-CELIV signal. This prevents the estimation of the carrier mobility as well as the bimolecular recombination reduction factor (β_L/β, where β_L is the Langevin type bimolecular recombination coefficient).[24] While some efforts have been directed to compensate the electric field inside the film by applying a time-dependent offset potential,[25] the inhomogeneous electric field inside the film[26] still extracts the photocarriers on inaccessibly short time scales. This limits the experimentally accessible time-resolution and renders the photo-CELIV technique inapplicable for measuring the carrier mobility

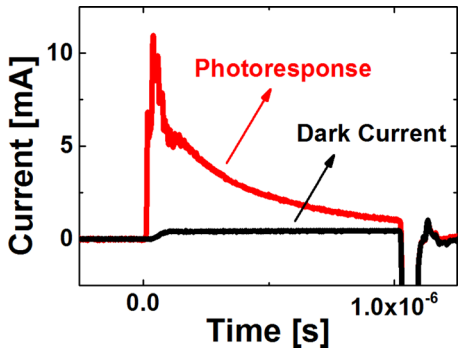

FIG. 2. Current transient signals of the photo-CELIV experiment. The extraction maximum, required for determination of the carrier mobility, is obscured by the time constant of the external circuit. This renders photo-CELIV inapplicable to measure the charge carrier mobility and recombination in these thin and efficient solar cells. However, the "flat" response of the dark current transient demonstrates the absence of doping induced equilibrium charge carriers, which is important for device performance and further simplifies the result interpretation of the RPV technique.

and recombination in thin, high mobility solar cells. Nevertheless, the measured dark-CELIV transients show a "flat" response (Fig. 2),[27,28] demonstrating the absence of equilibrium charge carriers, and hence the active layer of the solar cell is intrinsically undoped. Negligible doping allows simplified parameter estimation from the RPV technique[12] and is important for good device performance.

Since steady state injection current and photo-CELIV techniques were inapplicable in these operational devices, we employed RPV.[12] In this technique, transient photovoltage signals (plotted in Fig. 3(a)) are recorded at different load resistances of the oscilloscope ranging from 1 Ω to 1 MΩ. The temporal evolution of the transients originates from the competition between the photocurrent and the external current. The observed characteristic shoulders in the transients appear when all photogenerated electrons and/or holes are extracted from the film.[12] Therefore, these shoulders represent the charge carrier transit times (t_{tr}) from which the carrier mobilities are calculated. In the case of dispersive transport, the photovoltage shoulders are smoothed out; nevertheless, they can still be identified from the gradual change in transient signals recorded at various load resistances. In Fig. 3(a), it can be seen that the first photovoltage shoulder occurs at approximately 85 ns, corresponding to a mean faster carrier mobility of 2.5×10^{-3} cm^2/V s. This mobility is similar to that measured on a $PC_{71}BM$-only film using another RPV experiment (5.5×10^{-3} cm^2/V s) (see supplementary material[16]) and is comparable to previous SCLC mobility measurements on films of $PC_{71}BM$ (3.3×10^{-3} cm^2/V s).[29] Therefore, the first shoulder marks the mean electron mobility. The second shoulder in the transient photosignal occurs around 1.5 μs. The corresponding mean mobility is 1.5×10^{-4} cm^2/V s. This mobility is within the range reported in the past (5.4×10^{-5} cm^2/V s to 5.8×10^{-4} cm^2/V s) measured in unipolar (hole) SCLC studies on non-operational PTB7-only films,[18,29–31] using the same processing conditions. There has also been a report where numerical simulations were employed to reproduce the experimentally measured transient photocurrent dynamics of PTB7:$PC_{71}BM$ devices.[32] In the latter work, the best

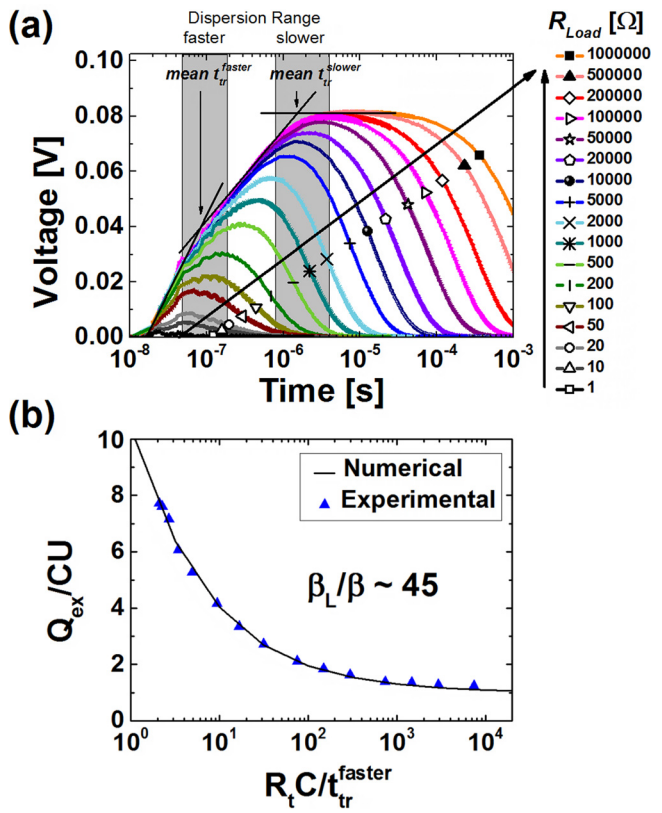

FIG. 3. (a) Load Resistance dependent PhotoVoltage (RPV) transients. The RPV technique allows to quantify the charge carrier mobility and bimolecular recombination coefficient in operational solar cells. The two observed photovoltage shoulders correspond to the faster (85 ns) and slower (1.5 μs) carrier transit times. The grey stripes highlight the dispersion ranges of carrier transit times. The corresponding estimated mean faster (electrons) and slower (holes) carrier mobilities are 2.5×10^{-3} cm^2/V s and 1.5×10^{-4} cm^2/V s. (b) The extracted charge (Q_{ex}) measured using high intensity RPV, shown as a function of the total circuit time constant (R_tC). By matching the experimental data points with numerical simulations the non-Langevin bimolecular recombination coefficient ($\beta_L/\beta \sim 45$) is directly estimated.

agreement between the simulations and experimental data was obtained by assuming a hole mobility of 10^{-4} cm^2/V s, which is consistent with our results. Interestingly, even though the two materials are blended in the device, their mobilities are similar to those measured in pristine films. The shoulders observed in the transient signals are not clearly pronounced as expected in the case of dispersive transport.[12] Therefore, the distribution of the carrier transit times (or mobilities) can be estimated directly from the breadth of the extraction shoulder. The dispersion range for electrons extends from 1×10^{-3} cm^2/V s to 4.5×10^{-3} cm^2/V s, while for holes the range extends from 5×10^{-5} cm^2/V s to 2.5×10^{-4} cm^2/V s. It should be noted that we have observed the charge carrier mobilities to be dependent on the PTB7 batch. This manifests in the absence of the first shoulder when the transit times are more balanced (<10 times). However, the shoulder corresponding to the extraction time of the slower carrier type (holes) is always distinct, which, importantly, is the critical parameter for the solar cell performance.[33,34]

Since charge transport is dependent on both charge carrier movement and recombination, we further studied the bimolecular carrier recombination process using high intensity RPV (HI-RPV).[35] In this experiment, the extracted charge

(Q_{ex}) is measured at high laser intensities as a function of the total circuit time constant (R_tC), where R_t is the sum of R_{load} and the series resistance of the circuit. Q_{ex} was obtained by integrating the transient photosignals (see supplementary material[16]). We note, that Q_{ex} was normalized by CU (where U is the built-in voltage) and R_tC by $t_{tr}^{\ faster}$ (where $t_{tr}^{\ faster}$ is the faster carrier t_{tr}) to compare the experimental data with the numerical predictions (the simulations are performed in normalized units). As shown in Fig. 3(b), the recombination rate was estimated by matching numerical simulations of Q_{ex}/CU versus $R_tC/t_{tr}^{\ faster}$ with experimental data points, and we found a non-Langevin recombination rate with a reduction factor β_L/β of $\sim$45 in the studied device. In the past, it was proposed that non-Langevin recombination could allow thicker active layers to be used when maximizing the light harvesting.[33] Strong non-Langevin behaviour suppresses the recombination losses and provides a significant advantage for the solar cell performance. This advantage is critically important at the maximum power point, where the effective voltage is very low (compared to the built-in voltage) for efficient carrier extraction. The active layer thickness and uniformity are the critical parameters when fabricating large scale panels using roll-to-roll high throughput solution processing.[36] In fact, PTB7:PC_{71}BM devices fabricated with 230 nm thick active layers still achieve PCEs of 6.1% with insignificant bimolecular recombination losses at short-circuit conditions (see supplementary material[16]). This is in sharp contrast to, for example, poly[*N*–9″-hepta-decanyl-2,7-carbazole-*alt*–5,5–(4′,7′-di-2-thienyl-2′,1′,3′-benzothiadiazole)] (PCDTBT):PC_{71}BM devices, where the PCE drops to 2.9% at the same active layer thickness due to significant bimolecular recombination losses (see supplementary material[16]).[37] The reason for the loss of performance in this blend is explained by the lower charge carrier mobilities and faster carrier recombination.[12,35]

In spite of a $\sim$15-fold imbalance in the carrier mobilities and the presence of dispersive transport, we still see IQEs near 100%. It was reported in the past that the required carrier mobility in several hundred nanometer thick active layers is on the order of 10^{-3} cm^2/V s.[38] However, the benefit of non-Langevin recombination allows for efficient charge extraction with much lower carrier mobilities (i.e., the lower edge of the dispersive slower carrier mobility is 5×10^{-5} cm^2/V s).

An interesting note regarding the recombination order relates to the previous Charge Extraction measurements by Rauh *et al.*[39] Higher than second order charge carrier decay rates were reported in PTB7:PC_{71}BM devices, which was attributed to trapped charge carriers that are protected from the recombination in a system with a partial donor–acceptor phase separation. A significant amount of long-lived ($> t_{tr}$ of slower carriers) traps is, however, not observed in our devices, since the extracted charge at large resistances is equal to CU (Fig. 3(b)).[35] Moreover, repetitive RPV transients measured at a low laser intensity prove the absence of long-lived traps in the studied efficient solar cells.[12] Bimolecular recombination has been widely recognized as the dominant recombination loss in efficient OSCs,[33,40,41] and second order recombination dynamics has been shown to prevail in optimized PTB7:PC_{71}BM blends using impedance spectroscopy[42] and Transient Photovoltage (TPV) measurements[43] at a 1 sun equivalent illumination intensity.

In summary, we have characterized the charge transport in efficient PTB7:PC_{71}BM organic solar cells. The RPV technique was employed to simultaneously measure mean electron and hole mobilities as well as the dispersion ranges for both types of carriers in operational and efficient solar cells, where other standard charge transport techniques, such as SCLC and photo-CELIV fail. Further work is required to identify the impact of dispersion range to the performance of organic solar cells. Measurements in operational devices demonstrate that a large photocurrent and high photovoltaic device performance can be achieved with a slower carrier mobility that is at least one order of magnitude lower compared to previously reported values. The reason why the low charge carrier mobility does not limit the device performance at short-circuit conditions is explained by significantly suppressed bimolecular recombination. The non-Langevin behaviour further prevents significant recombination losses at the maximum power point, which allows the use of thicker active layers for printing technologies and improved light harvesting.

A.P. is the recipient of an Australian Research Council Discovery Early Career Researcher Award (Project Nos. ARC DECRA DE120102271, UQ ECR59-2011002311, and UQ NSRSF-2011002734). A.K.P. is a recipient of an Australian Renewable Energy Agency (ARENA) Research Fellowship. A.A. and M.S. are funded by a University of Queensland International scholarship (UQI). P.M. and P.L.B. are University of Queensland Vice Chancellor's Senior Research Fellows. We acknowledge funding from the University of Queensland (Strategic Initiative-Centre for Organic Photonics and Electronics) and the Queensland Government (National and International Research Alliances Program). This work was performed in part at the Queensland node of the Australian National Fabrication Facility (ANFF-Q) – A company established under the National Collaborative Research Infrastructure Strategy to provide nano- and microfabrication facilities for Australia's researchers.

[1]A. Kokil, K. Yang, and J. Kumar, J. Polym. Sci. B: Polym. Phys. **50**, 1130 (2012).
[2]R. J. Kline and M. D. McGehee, J. Macromol. Sci. C: Polym. Rev. **46**, 27 (2006).
[3]R. Kline, M. McGehee, E. Kadnikova, J. Liu, and J. Fréchet, Adv. Mater. **15**, 1519 (2003).
[4]C. Goh, R. J. Kline, M. D. McGehee, E. N. Kadnikova, and J. M. J. Fréchet, Appl. Phys. Lett. **86**, 122110 (2005).
[5]T. M. Clarke, J. Peet, A. Nattestad, N. Drolet, G. Dennler, C. Lungenschmied, M. Leclerc, and A. J. Mozer, Org. Electron. **13**, 2639 (2012).
[6]A. Armin, G. Juška, M. Ullah, M. Velusamy, P. L. Burn, P. Meredith, and A. Pivrikas, Adv. Energy Mater. **4**, 1300954 (2014).
[7]S. Günes, A. Wild, E. Cevik, A. Pivrikas, U. S. Schubert, and D. A. Egbe, Sol. Energy Mater. Sol. Cells **94**, 484 (2010).
[8]N. Y. Canli, S. Günes, A. Pivrikas, A. Fuchsbauer, D. Sinwel, N. Sariciftci, Ö. Yasa, and B. Bilgin-Eran, Sol. Energy Mater. Sol. Cells **94**, 1089 (2010).
[9]A. Pivrikas, M. Ullah, T. Singh, C. Simbrunner, G. Matt, H. Sitter, and N. Sariciftci, Org. Electron. **12**, 161 (2011).
[10]A. Pivrikas, M. Ullah, H. Sitter, and N. S. Sariciftci, Appl. Phys. Lett. **98**, 092114 (2011).

[11]H. T. Nicolai, M. M. Mandoc, and P. W. M. Blom, Phys. Rev. B **83**, 195204 (2011).
[12]B. Philippa, M. Stolterfoht, P. L. Burn, G. Juška, P. Meredith, R. D. White, and A. Pivrikas, "The impact of hot charge carrier mobility on photocurrent losses in polymer-based solar cells," Sci. Rep. (to be published), e-print arXiv:1403.0311.
[13]A. Armin, G. Juška, B. W. Philippa, P. L. Burn, P. Meredith, R. D. White, and A. Pivrikas, Adv. Energy Mater. **3**, 321 (2013).
[14]Z. He, C. Zhong, S. Su, M. Xu, H. Wu, and Y. Cao, Nature Photon. **6**, 591 (2012).
[15]A. Armin, M. Velusamy, P. Wolfer, Y. Zhang, P. L. Burn, P. Meredith, and A. Pivrikas, ACS Photon. **1**, 173 (2014).
[16]See supplemental material at http://dx.doi.org/10.1063/1.4887316 for further details about RPV and HI-RPV measurements; SCLC mobility measurements; RPV transients in a $PC_{71}BM$-only device; Absorption spectra for IQE determination; n and k spectra; HI-RPV transients in the studied PTB7:$PC_{71}BM$ device; and J-V characteristics of 230 nm thick PTB7:$PC_{71}BM$ and PCDTBT:$PC_{71}BM$ devices.
[17]A. Armin, M. Velusamy, P. L. Burn, P. Meredith, and A. Pivrikas, Appl. Phys. Lett. **101**, 083306 (2012).
[18]Y. Liang, Z. Xu, J. Xia, S.-T. Tsai, Y. Wu, G. Li, C. Ray, and L. Yu, Adv. Mater. **22**, E135 (2010).
[19]M. A. Lampert and P. Mark, *Current Injection in Solids* (Academic Press, New York and London, 1970).
[20]H. Jin, A. Pivrikas, K. H. Lee, M. Aljada, M. Hambsch, P. L. Burn, and P. Meredith, Adv. Energy Mater. **2**, 1338 (2012).
[21]V. Mihailetchi, H. Xie, B. de Boer, L. Koster, and P. Blom, Adv. Funct. Mater. **16**, 699 (2006).
[22]D. A. M. Egbe, E. Tekin, E. Birckner, A. Pivrikas, N. S. Sariciftci, and U. S. Schubert, Macromolecules **40**, 7786 (2007).
[23]G. Adam, A. Pivrikas, A. M. Ramil, S. Tadesse, T. Yohannes, N. S. Sariciftci, and D. A. M. Egbe, J. Mater. Chem. **21**, 2594 (2011).
[24]G. Juška, N. Nekrašas, V. Valentinavicius, P. Meredith, and A. Pivrikas, Phys. Rev. B **84**, 155202 (2011).
[25]A. Baumann, J. Lorrmann, D. Rauh, C. Deibel, and V. Dyakonov, Adv. Mater. **24**, 4381 (2012).
[26]R. Österbacka, G. Juška, K. Arlauskas, A. J. Pal, K.-M. Källman, and H. Stubb, J. Appl. Phys. **84**, 3359 (1998).
[27]K. B. Krueger, P. E. Schwenn, K. Gui, A. Pivrikas, P. Meredith, and P. L. Burn, Appl. Phys. Lett. **98**, 083301 (2011).
[28]D. A. M. Egbe, G. Adam, A. Pivrikas, A. M. Ramil, E. Birckner, V. Cimrova, H. Hoppe, and N. S. Sariciftci, J. Mater. Chem. **20**, 9726 (2010).
[29]Z. He, C. Zhong, X. Huang, W.-Y. Wong, H. Wu, L. Chen, S. Su, and Y. Cao, Adv. Mater. **23**, 4636 (2011).
[30]H. Zhou, Y. Zhang, J. Seifter, S. D. Collins, C. Luo, G. C. Bazan, T.-Q. Nguyen, and A. J. Heeger, Adv. Mater. **25**, 1646 (2013).
[31]B. Carsten, J. M. Szarko, H. J. Son, W. Wang, L. Lu, F. He, B. S. Rolczynski, S. J. Lou, L. X. Chen, and L. Yu, J. Am. Chem. Soc. **133**, 20468 (2011).
[32]Z. Li, G. Lakhwani, N. C. Greenham, and C. R. McNeill, J. Appl. Phys. **114**, 034502 (2013).
[33]A. Pivrikas, H. Neugebauer, and N. Sariciftci, IEEE J. Sel. Top. Quant. Electron. **16**, 1746 (2010).
[34]M. Lenes, M. Morana, C. J. Brabec, and P. W. M. Blom, Adv. Funct. Mater. **19**, 1106 (2009).
[35]B. Philippa, M. Stolterfoht, R. White, M. Velusamy, P. L. Burn, P. Meredith, and A. Pivrikas, "Molecular weight dependent bimolecular recombination in organic solar cells," J. Chem. Phys. (submitted), e-print arXiv:1403.0972.
[36]F. C. Krebs, Sol. Energy Mater. Sol. Cells **93**, 394 (2009).
[37]S. Wakim, S. Beaupre, N. Blouin, B.-R. Aich, S. Rodman, R. Gaudiana, Y. Tao, and M. Leclerc, J. Mater. Chem. **19**, 5351 (2009).
[38]V. Petrova-Koch, R. Hezel, A. Goetzberge, D. Z. Zhu, Mühlbacher, M. Morana, M. Koppe, M. Scharber, D. Waller, G. Dennler, and C. Brabec, *High-Efficient Low-Cost Photovoltaics: Recent Developments* (Springer-Verlag, Berlin Heidelberg, 2008), p. 198.
[39]D. Rauh, C. Deibel, and V. Dyakonov, Adv. Funct. Mater. **22**, 3371 (2012).
[40]W. L. Leong, S. R. Cowan, and A. J. Heeger, Adv. Energy Mater. **1**, 517 (2011).
[41]S. Cowan, N. Banerji, W. Leong, and A. Heeger, Adv. Funct. Mater. **22**, 1116 (2012).
[42]A. Guerrero, N. Fernandez-Montcada, J. Ajuria, I. Etxebarria, R. Pacios, G. Garcia-Belmonte, and E. J. Palomares, J. Mater. Chem. A **1**, 12345 (2013).
[43]A. Foertig, J. Kniepert, M. Gluecker, T. Brenner, V. Dyakonov, D. Neher, and C. Deibel, Adv. Funct. Mater. **24**, 1306 (2014).